Development of synthetic salinity from remote sensing for the Columbia River plume

Sherry L. Palacios,[1] Tawnya D. Peterson,[1,2] and Raphael M. Kudela[1]

[1] The Columbia River plume (CRP) is an ecologically important source of nutrients, pollutants, and fresh water to the Oregon/Washington shelf. It is traditionally under-sampled, with observations constrained to ships or moorings. High-spatial- and temporal-resolution observations afforded by satellites would increase sampling if the plume could be quantitatively detected in the imagery. Two empirical algorithms are presented using data from the Moderate Resolution Imaging Spectroradiometer (MODIS) to estimate sea surface salinity in the region of CRP. Salinity cannot be detected directly, so a proxy for fresh water is employed. Light absorption by chromophoric dissolved organic matter (a_{CDOM}) is inversely proportional to salinity and linear because of conservative mixing of CDOM-rich terrestrial runoff with surrounding ocean water. To estimate synthetic salinity, simple linear (salinity versus a_{CDOM}) and multiple linear (salinity and temperature versus a_{CDOM}) algorithms were developed from in situ measurements of a_{CDOM} collected on the Coastal Ocean Processes–River Influences on Shelf Ecosystems cruises. These algorithms were applied to MODIS 250 m resolution data layers of sea surface temperature and absorption by colored dissolved and detrital matter (a_{CDM}) estimated at 350 nm and 412 nm from the Garver-Siegel-Maritorena model version 1 algorithm. Validation of MODIS-derived synthetic salinity with coincident in situ measurements revealed significant correlation during both downwelling (simple, $\beta_1 = 0.95$ and $r^2 = 0.89$; multiple, $\beta_1 = 0.92$ and $r^2 = 0.89$) and upwelling periods (simple, $\beta_1 = 1.26$ and $r^2 = 0.85$; multiple, $\beta_1 = 1.10$ and $r^2 = 0.87$) using the 412 nm data layer. Synthetic salinity estimated using the 350 nm data layer consistently overestimated salinity. These algorithms, when applied to a_{CDM} at 412 nm, enable synoptic observations of CRP not permitted by ships or moorings alone.

1. Introduction

[2] The Columbia River watershed spans 674,000 km^2 and includes parts of the northwestern U.S. and southwestern Canada. The mouth of the river lies at the border of the U.S. states of Washington and Oregon (46°N, 124°W). Approximately 77% of the fresh water flow to the NE Pacific Ocean, from San Francisco to the Strait of Juan de Fuca, comes from the Columbia River [*Hickey*, 1989]. Discharge varies from 3000–17,000 m^3 s^{-1} (averaging 7000 m^3 s^{-1} annually), and reaches a maximum freshet in the spring because of snowmelt [*Hickey*, 1998]. Flow of the Columbia River pulses tidally to the ocean where it becomes a buoyant plume [*Hickey*, 1989]. The forces of wind stress, Coriolis, and inertia influence the flow of the

Columbia River plume (CRP) as it exits the mouth. With southerly winds, downwelling conditions prevail and the plume flows northward along the Washington shelf. Northerly winds induce upwelling and the plume flows southward and offshore [*Hickey*, 1989]. It was widely accepted that the northward flow dominates in the winter and southward flow dominates in the summer. However, this canonical view of flow has recently been challenged [*Garcia Berdeal et al.*, 2002]. Even short-term (hours to days) oscillations in wind forcing can cause transient reversals in the typical seasonal flow patterns [*Garcia Berdeal et al.*, 2002; *Hickey*, 1998], with reversals more probable in summer than winter. *Thomas and Weatherbee* [2006] analyzed the variability of the CRP along the Washington and Oregon coastal margin over a period of 6 years (1998–2003) using Sea-viewing Wide Field-of-view Sensor imagery. The analysis included a supervised classification scheme using 5 channels of normalized water-leaving radiance (nL$_w$ at 412, 443, 490, 510 and 555 nm). Their observations confirmed the bimodal flow of the plume, but they lacked in situ measurements for a validation of ocean color products and could relate statistical patterns in the imagery but not geochemically describe those patterns.

[1]Ocean Sciences Department, University of California, Santa Cruz, California, USA.
[2]Now at Division of Environmental and Biomolecular Systems, Department of Science and Engineering, Oregon Health and Science University, Beaverton, Oregon, USA.

[3] The CRP supplies silicate, nitrate, trace metals, pollution, fresh water, and organic matter (both dissolved and particulate) to the Washington and Oregon shelves [*Aguilar-Islas and Bruland*, 2006; *Carpenter and Peterson*, 1989; *Hill and Wheeler*, 2002; *Kachel and Smith*, 1989; *Klinkhammer et al.*, 2000; *Landry et al.*, 1989; *McCarthy and Gale*, 1999]. Stratification caused by the fresh water lens and retention of nutrient-rich waters on the shelf promote phytoplankton growth in this ecologically important habitat for juvenile salmon [*De Robertis et al.*, 2005; *Morgan et al.*, 2005]. Therefore, identifying and tracking the plume is important for understanding the physical processes affecting the biology and chemistry of the region. Some constituents in the water clearly act as optical tracers of the plume as it flows away from the river mouth [*Thomas and Weatherbee*, 2006]. Plume-stimulated phytoplankton biomass, suspended inorganic and organic material (e.g., sediments), and chromophoric dissolved organic matter (CDOM) all have optical signals that may be useful for detecting and tracking the plume as it migrates along the Washington shelf or is absorbed into the California Current.

[4] Salinity presently cannot be directly detected using satellites at small regional scales (10s of km), but sensors are in development to estimate global salinity from space at spatial scales of 10s to 100s of km and temporal scales of 30 days or more between estimates [*Lagerloef et al.*, 2008]. Despite improvements in remotely detecting salinity, most of the world's river plumes are too small and temporally dynamic to discern in the coastal environment using these new satellites. Existing ocean color sensors (e.g., Moderate Resolution Imaging Spectroradiometer (MODIS)) can detect CDOM, which can be used as an optical tracer of river plumes in coastal margins [*Binding and Bowers*, 2003; *Callahan et al.*, 2004; *Hu et al.*, 2004; *Johnson et al.*, 2003; *Vasilkov et al.*, 1999] at spatial and temporal scales relevant to their dynamic processes.

[5] The unique optical character of CDOM in river water [*Chen et al.*, 2004; *Hernes and Benner*, 2003] can be employed as a proxy for low-salinity water nearshore [*Del Vecchio and Subramaniam*, 2004; *Johnson et al.*, 2003]. CDOM is operationally defined as the substance that passes through a 0.2 μm filter and absorbs light strongly from the ultraviolet to ~450 nm [*Kirk*, 1994; *Babin et al.*, 2003]. It is a fraction of the total DOM pool and can be important in biogeochemical processes [*Mopper and Kieber*, 2002] as well as an optical tracer. CDOM contributes to the quality and quantity of light leaving the sea surface and its variability in natural waters can be used to distinguish water types [*Bricaud et al.*, 1981; *Carder et al.*, 1989]. The bulk CDOM pool in river plumes is enriched in tannins and lignins which contain highly absorbing aromatic rings [*Blough and Del Vecchio*, 2002]. This terrestrially derived CDOM absorbs light strongly at 350 nm and has a different optical character than marine CDOM which has few, if any, aromatic rings and absorbs weakly at 350 nm. The sources of CDOM in river plumes can be degraded vegetative material in the watershed; the product of phytoplankton and bacterial metabolism in the river, estuary, or plume after it exits the river mouth; or leachate from soils and estuarine sediments [*Blough and Del Vecchio*, 2002; *Klinkhammer et al.*, 2000]. CDOM at the land-sea interface is generally terrestrially derived and loses its distinguishing character as

it mixes conservatively with the old, "dirty laundry" CDOM of the open ocean [*Siegel et al.*, 2002; *Stedmon and Markager*, 2003]. It is the difference in optical character between terrestrial and marine derived CDOM that can be exploited to optically detect low-salinity plumes in nearshore environments [*Vasilkov et al.*, 1999; *Johnson et al.*, 2003; *Conmy et al.*, 2004; *Del Vecchio and Subramaniam*, 2004].

[6] Remote sensing in the coastal environment affords a synoptic view that would be costly or not possible using shipboard measurements alone. However, ground truth measurements are needed, particularly in an environment as dynamic as the Columbia River plume. This study measures those in situ optical properties and is the first to relate salinity to optical properties to identify this water mass on the Washington and Oregon shelf. The objectives of this study were (1) to develop empirical algorithms to estimate low-salinity water in the region of the Columbia River plume and (2) to apply the algorithms to 250 m resolution MODIS data products. The study was conducted during the Coastal Ocean Processes–River Influences on Shelf Ecosystems (CoOP-RISE) cruises in June 2004, June 2005, August 2005, and June 2006 at the mouth and surrounding areas of the Columbia River.

2. Methods
2.1. In Situ Sample Collection

[7] Four research cruises were conducted aboard two vessels, the R/V *Wecoma* and R/V *Point Sur*, on the Washington and Oregon shelf in the vicinity of the CRP during June to July 2004, May to June 2005, August 2005, and May to June 2006. Hereafter the cruises will be referred to as June 2004, June 2005, August 2005, and June 2006. The study area was contained within a region bounded by 44.7°N and 48.5°N latitude and 123.5°W and 125.2°W longitude (Figure 1). Three of the cruises were scheduled to occur during maximum river discharge in the spring and one during reduced flow in the late summer (Figure 2) (USGS, discharge at the Beaver Army Terminal, Quincy, OR).

[8] Light absorption by CDOM (a_{CDOM}) was measured from discrete water samples collected near the surface from the CTD rosette and the underway water stream. The underway system collected water at 4 m in 2004 and at 2 m in 2005 and 2006. Temperature and salinity were recorded at the time of water collection. Each sample was filtered through a 0.2 μm Nuclepore® polycarbonate filter, sealed in a polypropylene vial, and stored in the dark at 4°C until it was processed (within six weeks) in the lab at University of California, Santa Cruz. CDOM optical properties are stable for up to four months if stored this way [*Johannessen et al.*, 2003]. Absorbance (A) was measured on a Cary UV-visible spectrophotometer (300–800 nm with 0.5 nm resolution) using a 0.1 m path length quartz cuvette. A Millipore Q-water blank was subtracted from these values and spectral absorption (a) was calculated using equation (1) [*Kirk*, 1994]

$$a_{\mathrm{CDOM}}(\lambda) = \frac{2.303 * \left(A_{(\lambda)} - A_{(750)}\right)}{0.1} \qquad (1)$$
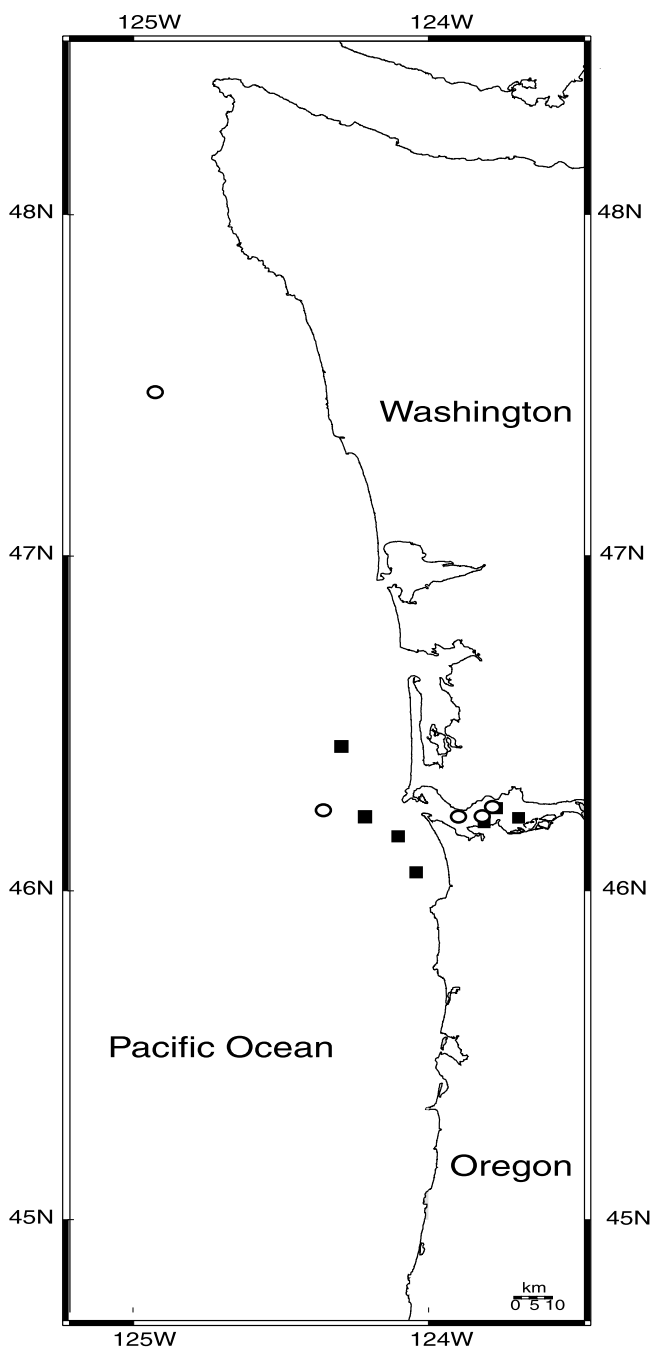
Figure 1. Study area. Washington and Oregon, United States shelf. Validation stations for 2004 (squares) and 2005 (circles).

[9] The value 2.303 is the correction factor converting log (10) to natural log, $A_{(750)}$ is subtracted from all values of A to account for scattering by small particles, and 0.1 m is the cuvette path length to give units m^{-1} for absorption. Light absorption at wavelength 350 nm was used in the analysis because terrestrially derived CDOM absorbs strongly at this wavelength because of tannins and lignins [*Hernes and Benner*, 2003]. This terrestrially derived CDOM acts as a tracer for fresh water on the shelf because CDOM concen-

tration is inversely proportional to salinity and its conservative decrease is a result of mixing.

2.2. Statistical Models

[10] Two empirical algorithms were developed for each cruise from the a_{CDOM} measurements collected in situ. The first algorithm ("simple model") was a simple linear regression testing salinity versus a_{CDOM} at 350 nm. The second algorithm ("multiple model") was a multiple linear regression testing salinity and temperature versus a_{CDOM} at 350 nm. Temperature was included in the multiple model to account for the possible contrast in temperature in river water from oceanic water, particularly because upwelling (represented by cool temperatures) is a dominant process in this region. An additional reason was to tune the salinity estimate to the CRP and away from the "false plumes" of nearby estuaries that may have had different native temperatures. A critical p-value of 0.05 was used to determine significance. These tests were conducted for each cruise, and then a multivariate analysis of covariance (MANCOVA) was used to determine differences among cruises. Statistical tests were computed using the MATLAB Statistics Toolkit (The MathWorks, Inc.).

2.3. Satellite Analysis
2.3.1. Data Collection

[11] During the 3 year study period, only 5 days out of a total of 95 cruise days were completely clear of clouds over the entire Oregon and Washington shelf. Of these 5 clear days, 2 days were selected that had sufficient shipboard and mooring data to compare in situ measurements of salinity to satellite derived estimates of salinity. These 2 days represented a period of wind driven oceanographic downwelling (21 July 2004) and oceanographic upwelling (25 August 2005) (Figure 3). In addition to these 2 clear days used in the salinity analysis, a subset of images from partly cloudy days was used to evaluate how well the satellite-derived estimate of light absorption by dissolved and detrital matter (a_{CDM}) fit to in situ, shipboard measurements of a_{CDOM}. Partly cloudy scenes were used when the region in the image matching the in situ collection location was clear of clouds or edge effects of clouds. Of 14, partially clear days in June 2004 and August 2005, only 4 in 2004 and 3 in 2005 met the requirements for comparison (11, 12, 17, and 21 July 2004 and 22, 23, and 25 August 2005).

[12] Level 0 MODIS swaths occupying the region 40° to 50°N and 128° to 123°W for the study days were downloaded from LAADS Web (Goddard Space Flight Center, Level 1 and Atmosphere Archive and Distribution System). These data were processed to Level 2 geophysical products using SeaDAS (version 5.1) with the default settings of the NASA/Goddard Ocean Biology Processing Group (OBPG) using a two wavelength (1240 and 2130 nm) atmospheric correction (B. A. Franz et al., MODIS land bands for ocean remote sensing applications, paper presented at 18th Ocean Optics Meeting, NASA, Montreal, Canada, 2006). Data were projected using a sinusoidal projection at 250 m resolution and subsetted to the region of the Oregon and Washington shelf bounded by 44.7° to 48.5°N and 123.4° to 125.2°W. The data layers acquired and processed in this study included sea surface temperature (SST) and light absorption by colored dissolved and detrital matter at
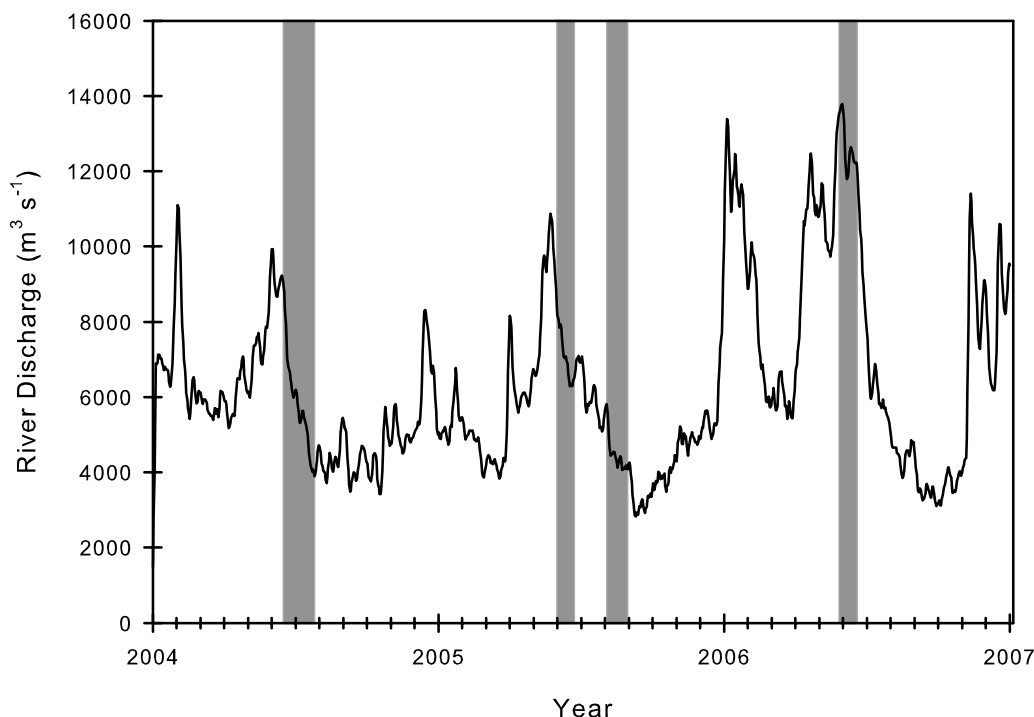
Figure 2. River discharge. Discharge of the Columbia River during the study period (5 day running averages). Measured at the Beaver Army Terminal, Quincy, Oregon, upstream of the Columbia River mouth. Volume reported as m^3 s^{-1}. Cruise dates noted by shaded area.

412 nm ($a_{dg}(\lambda)$) using the Garver-Siegel-Maritorena model version 1 (GSM01) [*Maritorena et al.*, 2002], Quasi-Analytical Algorithm (QAA) [*Lee et al.*, 2002], and Carder [*Carder et al.*, 1999] algorithms. Estimates of a_{dg} 350 nm were calculated using equation (2) [*Twardowski et al.*, 2004]:

$$a_\lambda = a_{\lambda 0} * \exp(s(\lambda_0 - \lambda)) \qquad (2)$$

where λ_0 equals 412; λ equals 350; and the spectral slope parameter, s, was 0.0206 for GSM01, 0.015 for QAA, and 0.022 for the Carder algorithm, the standard parameter values used by SeaDAS. Although the data used for these analyses (SST and $a_{dg}(\lambda)$) are at a native resolution of 1 km (nadir), SeaDAS applies a bilinear cubic interpolation to create pseudo-250 m resolution data; the algorithms then use the true 250 m resolution data at 645 nm and 500 m resolution data at 469 nm and 555 nm wavelengths to interpolate the 250 m resolution for the other wavelengths (B. A. Franz et al., MODIS land bands for ocean remote sensing applications, paper presented at 18th Ocean Optics Meeting, NASA, Montreal, Canada, 2006).

2.3.2. The a_{CDOM} Versus a_{CDM} and Algorithm Comparison

[13] The three satellite algorithms were carefully evaluated to determine which one had the best fit of in situ a_{CDOM} at 412 nm to satellite-derived a_{dg} 412 nm. Sediment and other colored detrital material influence the a_{dg} measurement; the goal was to quantify the error due to the presence of this material and to choose the algorithm with the best fit for a_{CDOM} for use in the salinity estimate. Shipboard measurements of a_{CDOM} were collected within

1 hour of the satellite overpass on each of the 7 days in 2004 and 2005 identified above (locations not shown). Diverse water types were sampled in 2004, though less so in 2005 because of the limits of available satellite imagery. The imagery was subsetted to a 4 by 4 pixel box (10^6 m^2) centered on the in situ sample location. The mean a_{dg} 412 nm value of this 4 by 4 pixel box was calculated for each scene for each of the three satellite algorithms. The in situ a_{CDOM} at 412 nm was the independent variable and these a_{dg} 412 nm estimates for each algorithm were the dependent variables in tests of simple linear regression with ANOVA. The slopes from the different regression tests were compared using a MANCOVA. A critical p-value of 0.05 was used to determine significance.

[14] Careful evaluation of the GSM01, QAA, and Carder algorithms revealed that in June 2004 in the region of the CRP, GSM01 had greater fidelity between in situ a_{CDOM} and satellite derived a_{CDM} with respect to fit, slope, and intercept (Table 1). The slopes for GSM01 and Carder were different in 2004 (F = 2.35, DFn = 1, DFd = 4, p = 0.04). In August, there was the expected trend between a_{CDOM} and a_{dg}, but no significant fit for any of the algorithms and so they could not be compared to each other. This lack of fit may have been the result of high turbidity, but more likely a result of low sample size exacerbated by the narrow range of a_{CDOM} values used in the comparison. We decided to restrict the salinity analysis of this study to the MODIS-derived data layers from the GSM01 algorithm for both years with the understanding that the overestimate observed was likely due to the presence of detrital and colored particles contributing to the a_{dg} measurement. As a result of this offset, synthetic salinity estimates have the potential
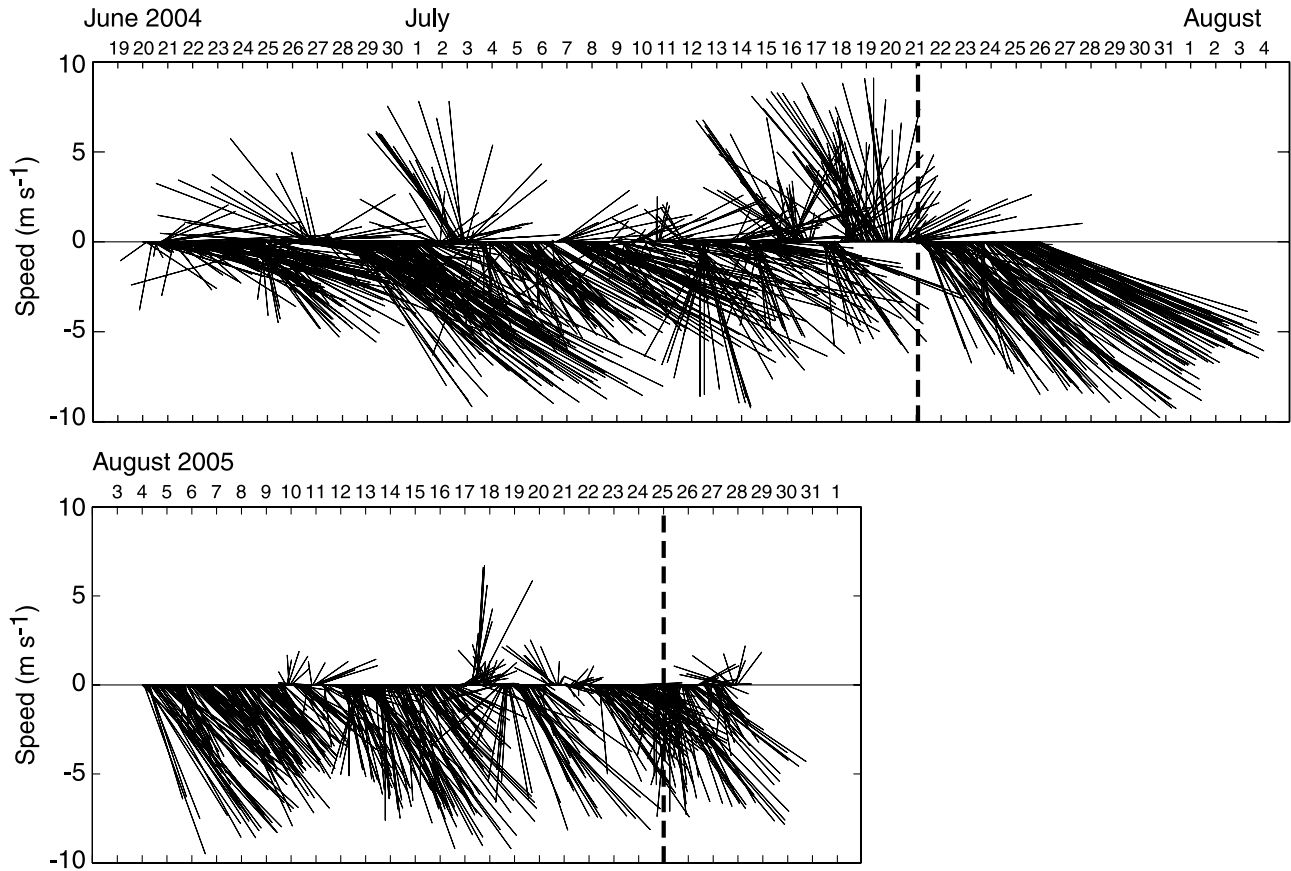
Figure 3. Wind vectors. Speed and direction of wind flow at the Columbia River mouth during the study periods in (a) 2004 and (b) 2005. Dashed lines represent date of satellite image capture and subsequent analysis. Note that 21 July 2004 was a period of downwelling-favorable winds and 25 August 2005 a period of upwelling-favorable winds.

to be negative if the a_{dg} estimate exceeds the parameters in the synthetic salinity model.

2.3.3. Synthetic Salinity Estimates

[15] Synthetic salinity was computed by inverting the in situ linear regression models to solve for salinity. The MODIS-derived data layers (250 m resolution GSM01 a_{dg} at 350 nm and 412 nm) were used as the inputs for a_{CDOM} and the SST data layer as the input for temperature (for the multiple algorithm). Both GSM01 a_{dg} 412 nm and the estimated values for GSM01 a_{dg} 350 nm were used to calculate synthetic salinity in order to determine if the a_{dg} 412 nm data layer was sufficient to accurately predict salinity, or if the derived data layer was needed since the underlying models were developed using a_{CDOM} at 350 nm. The simple model computed synthetic salinity using equation (3):

$$\text{synthetic salinity} = \frac{a_{CDOM} - \beta_0}{\beta_1} \quad (3)$$

where β_0 and β_1 are the intercept and regression coefficients, respectively. The standard equation (4) for the multiple model was inverted to solve for synthetic salinity:

$$\text{synthetic salinity} = \frac{a_{CDOM} - \beta_0 - \beta_2(\text{temperature})}{\beta_1} \quad (4)$$

where β_2 is the second regression coefficient. The empirical algorithms developed for each cruise were only applied to imagery collected during the respective cruise. Four estimates of synthetic salinity were computed for each date: simple synthetic salinity using a_{dg} 350 nm and 412 nm and multiple synthetic salinity using a_{dg} 350 nm and 412 nm.

2.4. Validation

[16] In situ measurements of salinity were compared to estimates of synthetic salinity to validate the robustness of the underlying empirical models. Several independent sources of in situ salinity measurements were used in the validation: underway shipboard measurements from the R/V *Wecoma* and R/V *Point Sur*, M/V *Forerunner*, CoOP-RISE moorings located on the shelf, and Columbia River Estuary moorings immediately within the river mouth (Table 2). For comparison of in situ and remotely sensed data, the mean of 4 minutes of salinity data (2 minute intervals centered at the time of the satellite overpass) was used as salinity data for the mooring and shipboard sources. Synthetic salinity from the remote sensing layers was selected using a 4 by 4 pixel box (10^6 m^2) centered on the in situ site. Pixels influenced by land were flagged using the SST and a_{dg} 412 nm bands and removed. The remaining pixels were used to compute the mean synthetic salinity value in this 10^6 m^2 box. These mean values were used in a

Table 1. Validation of in Situ a_{CDOM} (412 nm) Surface Measurements With MODIS-Derived a_{dg} 412 nm Estimates for the Three Algorithms GSM01, QAA, and Carder[a]

| | | | Results of Regression Analysis | | |
Estimate	r^2	n	β_1	β_0	p
			2004		
GSM01	0.98	4	1.4	−0.23	<0.05
QAA	0.59	4	0.67	−0.05	not significant
Carder	0.92	4	0.75	−0.09	<0.05
			2005		
GSM01	0.95	3	2.5	−0.59	not significant
QAA	0.95	3	2.4	−0.59	not significant
Carder	0.27	3	1.4	−0.21	not significant

[a]β_1 = regression coefficient, β_0 = intercept, and $p \leq 0.05$ is significant.

test of simple linear regression (in situ salinity versus synthetic salinity) to determine a fit between measured and modeled salinity and to estimate error. A critical p-value of 0.05 was used to determine significance.

3. Results

3.1. Field Setting

[17] River discharge varied seasonally, with a trend of relatively high flow during the spring and reduced flow in the late summer and autumn (Figure 2). This seasonal pattern is typical for the Columbia River. High flows are due to runoff of snowmelt in the watershed and can vary in timing annually. Maximum discharge preceded the June 2004 and June 2005 cruises, and was concurrent with the June 2006 cruise. Peak discharge in June 2006 was 50% greater than peak discharge in 2004 and 2005, which were similar to each other. A delay in the onset of upwelling-favorable winds in 2005 resulted in a period in June with no upwelling and anomalously warm waters throughout the northern California Current system; however, by our August cruise (Figure 3), strong upwelling-favorable conditions were present [*Hickey et al.*, 2006; *Kudela et al.*, 2006]. Anomalously warm SST in June 2005 decreased the gradient in temperatures between plume and offshore water, which may have influenced mixing of the plume with surrounding marine waters.

[18] Light absorption by CDOM was linear and inversely proportional to salinity (Figure 4). The relationship of salinity to a_{CDOM} at 350 nm in the simple model was significant for discrete water samples measured for each of the cruises (Table 3). When the cruises were compared to each other using MANCOVA, the slopes were found to be statistically different (F = 22.41, DFn = 3, DFd = 171, p < 0.001), and therefore intercepts could not be compared among all of the cruises. When the June cruises from all years were compared to each other, the relationship between salinity and a_{CDOM} at 350 nm was similar between 2005 and 2006, but not 2004 (F = 3.64, DFn = 2, DFd = 140, p = 0.03). Nevertheless, June values were pooled to produce a "universal" statistical relationship of salinity to light absorption by CDOM for the spring freshet, with the understanding that natural variability exists among years. This universal synthetic salinity model followed the same trend as the statistically significant models from individual cruises

and may be useful to estimate synthetic salinity on the shelf in future work. The relationship of salinity and temperature to a_{CDOM} at 350 nm in the multiple model was significant for discrete water samples measured for each of the cruises (Table 4).

### 3.2. Observations During a Downwelling Period (21 July 2004)

[19] The CRP formed a coherent feature on the Washington shelf, north of the river mouth in the image dated 21 July 2004 (Figures 5 and 6). There was a distinct bolus of what appeared to be fresh water west of the river mouth. The satellite overpass occurred 4.5 h after maximum ebb tide during a period of very low spring tides. River discharge averaged 3816 m^3 s^{-1} this day. The river plume appears to extend northward along the shelf which may be remnant plume water from previous days during this downwelling period.

[20] The plume can be clearly distinguished in both the simple and multiple model estimates for synthetic salinity using GSM01 a_{dg} 350 nm (Figure 5) and GSM01 a_{dg} 412 nm (Figure 6). The simple and multiple models corresponded closely to each other for each data layer (a_{dg} 350 nm: β_1 = 1.006; r^2 = 0.99; $p \leq 0.05$; a_{dg} 412 nm: β_1 = 1.015; r^2 = 0.99; $p \leq 0.05$, where β_1 is the slope of the regression and β_0 is the intercept). Synthetic salinity estimates of the simple algorithm were approximately 0.6% less than estimates of the multiple algorithm using a_{dg} 350 nm and 1.5% less using a_{dg} 412 nm. In the simple algorithm and using a_{dg} 350 nm (Figure 5a), synthetic salinity estimates ranged from −47.0 in the estuary to 36.2 offshore. The nascent plume at the mouth of the river had synthetic salinity that ranged from 5.2 to 13.0 and plume axis salinities ranging from −5.6 to 10.5. The edges of the plume were defined by a steep gradient in synthetic salinity from 6.3 to 22.9 over a distance less than 4 km. In the simple algorithm and using a_{dg} 412 nm (Figure 6a), synthetic salinity estimates ranged from 0.6 in the estuary to 37.4 offshore. Synthetic salinity at the river mouth ranged

Table 2. Date, Data Source, and Location for in Situ, Ground Truth Salinity Measurements[a]

Data Source	Latitude (°N)	Longitude (°W)	Depth (m)
	21 July 2004		
R/V *Wecoma*	46.200	123.806	4
R/V *Point Sur*	46.242	124.260	4
RISO	46.053	124.101	1
RINO	46.437	124.301	1
RICE	46.167	124.195	1
Grays Point	46.262	123.767	6.4
CBNC3	46.210	123.714	6.5
	25 August 2005		
R/V *Wecoma*	47.493	124.912	2
R/V *Point Sur*	46.251	124.360	4
M/V *Forerunner*	46.233	123.872	1
Grays Point	46.262	123.767	6.4
CBNC3	46.210	123.714	6.5

[a]Coastal Ocean Processes–River Influences on Shelf Ecosystems temporary deployed moorings include RISO, RINO, and RICE (courtesy, E. Dever (personal communication, 2008)). Columbia River Estuary measurements include moorings (Grays Point and CBNC3) and shipboard measurements on the M/V *Forerunner* (courtesy, A. Baptista (personal communication, 2008)). RISO, RISE South; RINO, RISE North; RICE, RISE Central; CBNC3, Cathlamet Bay North Channel 3.
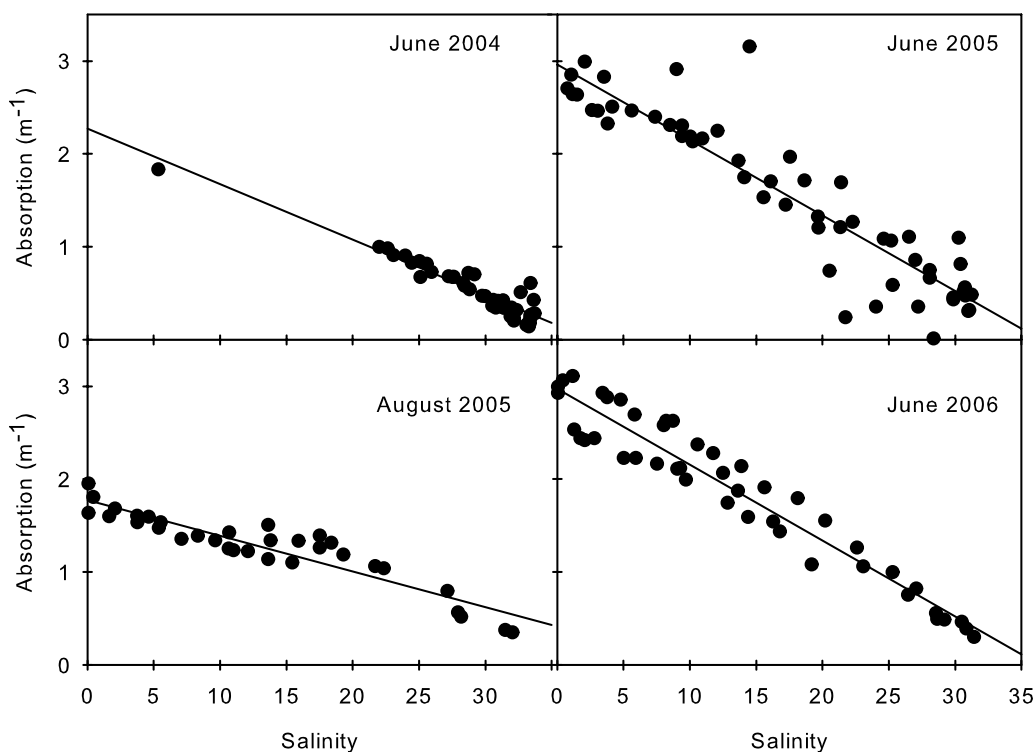
Figure 4. In situ salinity model. Relationship of salinity to light absorption at 350 nm for discrete water samples collected during the June 2004, June 2005, August 2005, and June 2006 Coastal Ocean Processes–River Influences on Shelf Ecosystems (CoOP-RISE) cruises. Light absorption at 350 nm was inversely related to salinity at each sample period. See Table 3 for statistics.

from 21.8 to 31.9 and plume axis salinities ranged from 21.8 to 27.9. The edges of the plume were defined by a fairly steep gradient in synthetic salinity over less than 4 km from 28.6 to 31.3. In the multiple algorithm and using a_{dg} 350 nm (Figure 5b), synthetic salinity ranged from −47.3 in the estuary to 38.0 offshore. The mouth of the plume ranged from −7.9 to 14.1 and along the plume axis had a synthetic salinity of −7.3 to 9.8. The edges of the plume had a steep gradient from 9.9 to 22.7. In the multiple algorithm and using a_{dg} 412 nm (Figure 6b), synthetic salinity estimates ranged from 0.7 in the estuary to 37.4 offshore. The mouth of the plume ranged from 20.5 to 31.0 and along the plume

axis had a synthetic salinity of 20.7 to 27.5. The edges of the plume ranged from 24.7 to 31.9.

3.3. Observations During an Upwelling Period (25 August 2005)

[21] The CRP was a diffuse feature on the Oregon and Washington shelf in the image dated 25 August 2005 (Figures 7 and 8). The CRP was only faintly present west and south of the river mouth. The satellite overpass occurred 3.5 h following maximum ebb tide during the neap tide, so the tidal range was very small. River discharge averaged 3852 m^3 s^{-1} this day, similar to the flow on 21 July 2004. This was a period of upwelling-favorable winds and the plume appeared to form a disjointed fan of water near and

Table 3. Results of Simple Linear Regression to Test the Relationship of Salinity to a_{CDOM} at 350 nm for Discrete Water Samples Collected Within and Outside of the Columbia River Plume in June 2004, June 2005, August 2005, June 2006, and all June Cruises Pooled[a]

	Results of Regression Analysis				
Cruise	r^2	n	β_1	β_0	p
June 2004	0.90	46	−0.06	2.27	<0.05
June 2005	0.85	55	−0.08	2.96	<0.05
August 2005	0.87	33	−0.04	1.77	<0.05
June 2006	0.93	45	−0.08	2.97	<0.05
Universal June	0.92	146	−0.08	2.95	<0.05

[a]β_1 = regression coefficient/slope, β_0 = intercept, and p ≤ 0.05 is significant.

Table 4. Results of Multiple Linear Regression to Test the Relationship of Salinity and Temperature to a_{CDOM} at 350 nm for Discrete Water Samples Collected Within and Outside of the Columbia River Plume in June 2004, June 2005, August 2005, June 2006, and All June Cruises Pooled[a]

	Results of Regression Analysis				
Cruise	r^2	n	β_1	β_2	β_0	p
June 2004	0.90	46	−0.06	0.01	2.09	<0.05
June 2005	0.85	55	−0.08	−0.13	5.00	<0.05
August 2005	0.87	33	−0.07	−0.12	4.42	<0.05
June 2006	0.96	45	−0.08	0.20	−0.17	<0.05
Universal June	0.92	146	−0.08	0.02	2.67	<0.05

[a]β_1 = regression coefficient for salinity, β_2 = regression coefficient for temperature, and β_0 = intercept; p ≤ 0.05 is significant.
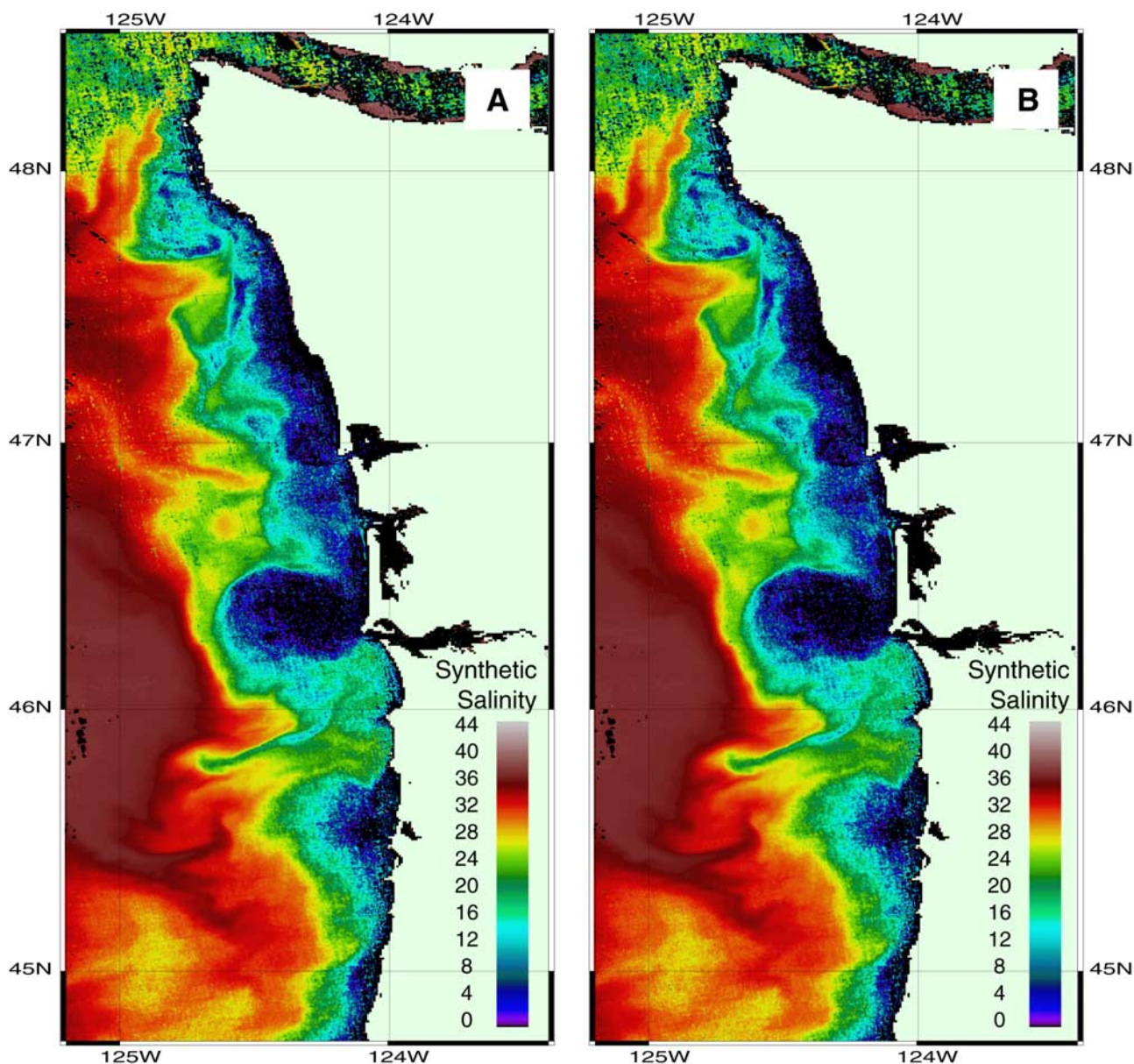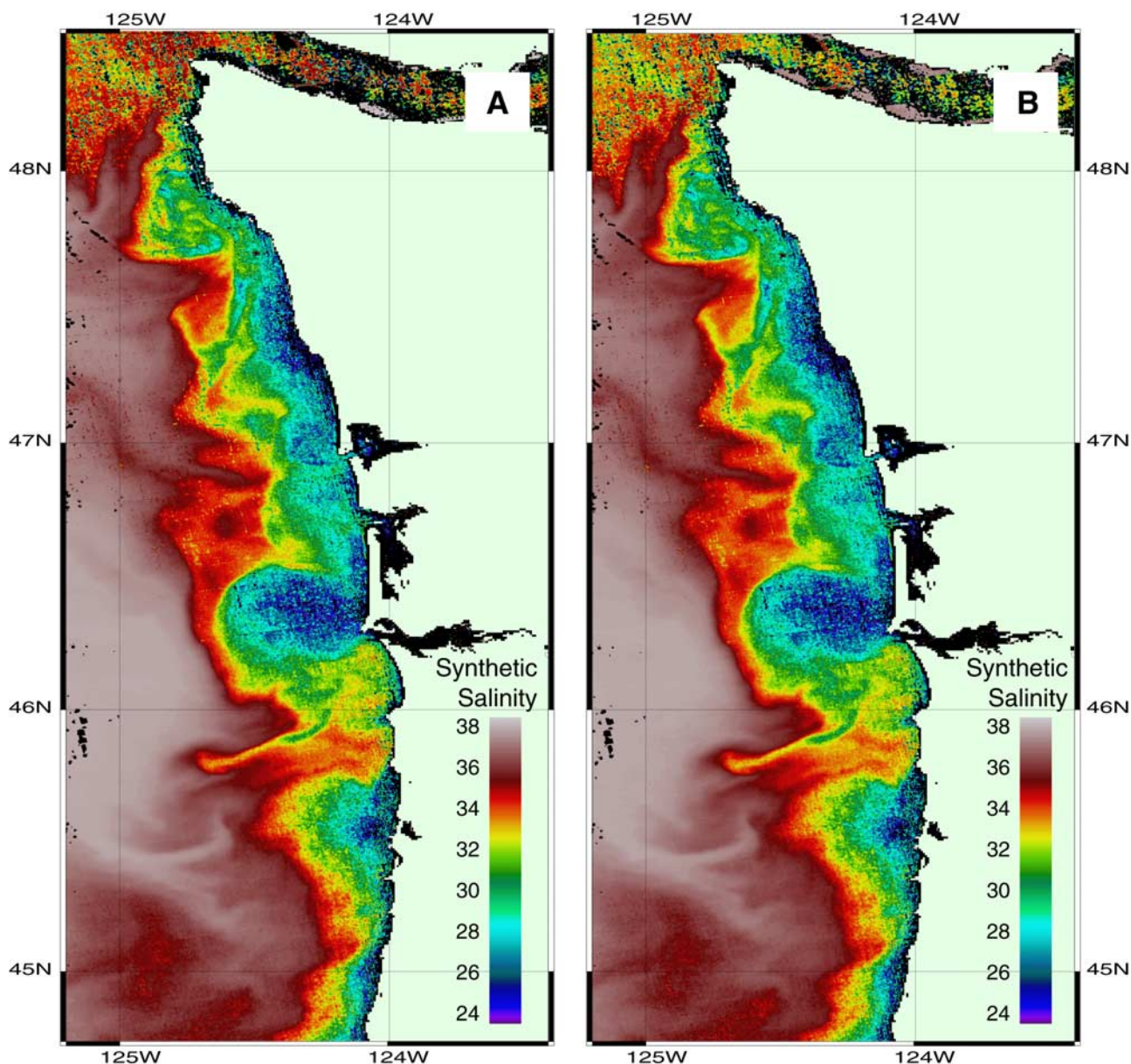
Figure 5. Synthetic salinity. Estimates of sea surface salinity for 21 July 2004, a period of downwelling oceanographic conditions. (a) Simple algorithm showing salinity versus a_{CDOM} at 350 nm and (b) multiple algorithm showing salinity and temperature versus a_{CDOM} at 350 nm. Satellite products used in analysis included the 250 m MODIS data layers for sea surface temperature and GSM01 a_{dg} 350 nm.

southward of the river mouth, where it was absorbed into what appeared to be the California Current.

[22] The simple and multiple algorithm estimates of synthetic salinity on the shelf did not closely correspond to each other in either the simple or multiple model estimates for synthetic salinity using GSM01 a_{dg} 350 nm (Figure 7) and GSM01 a_{dg} 412 nm (Figure 8). Estimates for synthetic salinity using the simple model overestimated values compared to the multiple model (a_{dg} 350 nm: $\beta_1 = 0.53$; $r^2 = 0.89$; $p \leq 0.05$; a_{dg} 412 nm: $\beta_1 = 0.48$; $r^2 = 0.54$; $p \leq 0.05$). Synthetic salinity estimates of the simple algorithm were approximately 53% more than estimates of the multiple algorithm using a_{dg} 350 nm and 48% more using a_{dg} 412 nm. In the simple algorithm and using a_{dg}

350 nm (Figure 7a), synthetic salinity estimates ranged from -52.0 in the estuary to 39.5 offshore. The river mouth had synthetic salinity that ranged from 9.3 to 21.6 and plume axis salinities ranging from 16.2 to 21.3. The edges of the plume were not well defined and ranged in synthetic salinity from 17.7 to 24.0 over a distance greater than 10 km. In the simple algorithm and using a_{dg} 412 nm (Figure 8a), synthetic salinity estimates ranged from 0.6 in the estuary to 42.8 offshore. Synthetic salinity at the river mouth ranged from 31.2 to 36.2 and plume axis salinities ranging from 29.9 to 37.5. The edges of the plume gradually transitioned from 36.4 to 38.5. In the multiple algorithm and using a_{dg} 350 nm (Figure 7b), synthetic salinity estimates ranged from -53.9 in the estuary to 31.3 offshore. The mouth of the
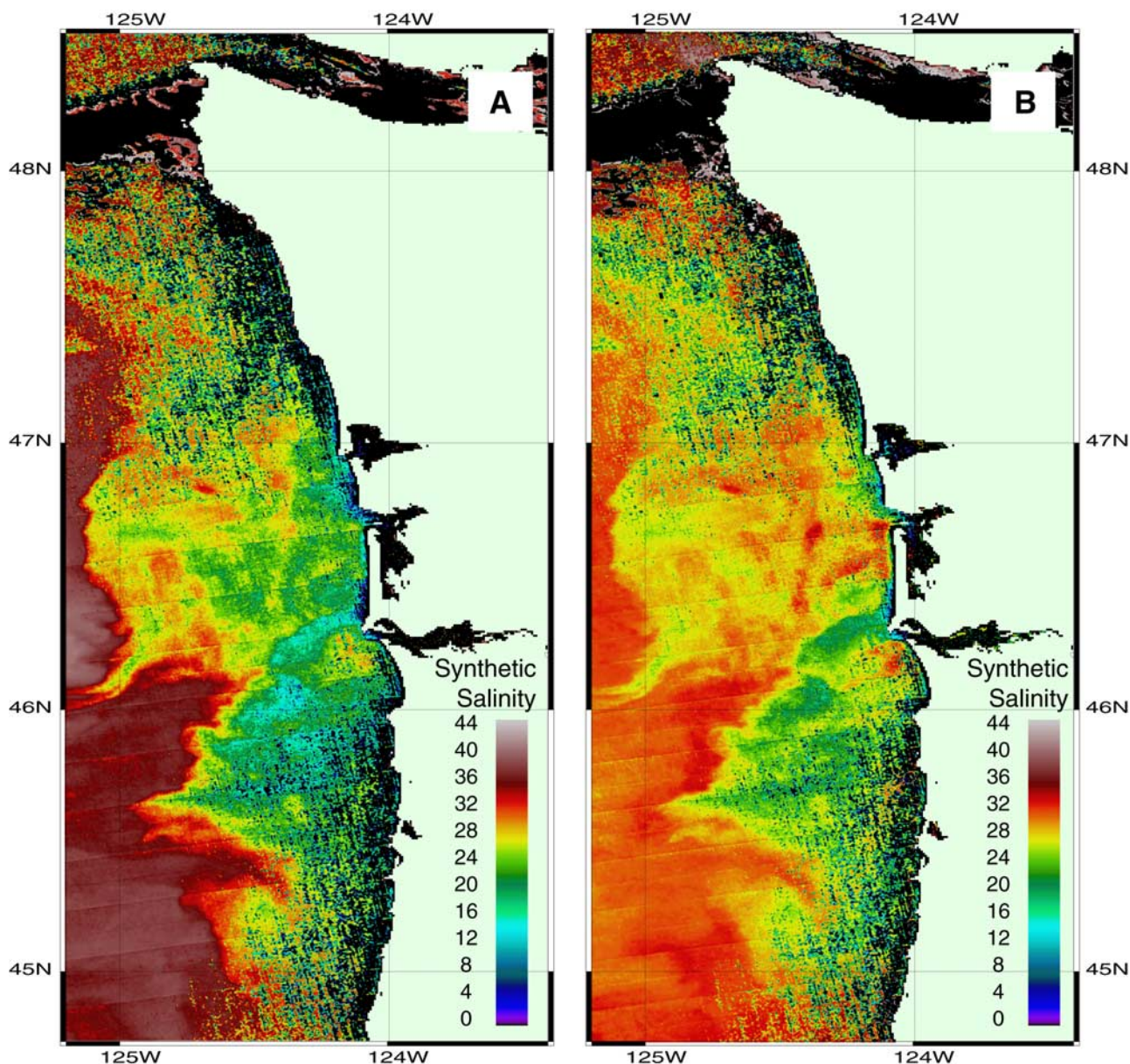
Figure 6. Synthetic salinity. Estimates of sea surface salinity for 21 July 2004, a period of downwelling oceanographic conditions. (a) Simple algorithm showing salinity versus a_{CDOM} at 412 nm and (b) multiple algorithm showing salinity and temperature versus a_{CDOM} at 412 nm. Satellite products used in analysis included the 250 m MODIS data layers for sea surface temperature and GSM01 a_{dg} 412 nm.

plume ranged from 5.22 to 15.9 and along the plume axis had a synthetic salinity of 14.5 to 24.8. The edges of the plume gradually decreased from 20.6 to 26.9. In the multiple algorithm and using a_{dg} 412 nm (Figure 8b), synthetic salinity estimates ranged from 2.9 in the estuary to 32.7 offshore. The mouth of the plume ranged from 24.5 to 28.6 and along the plume axis had a synthetic salinity of 27.1 to 33.4. The edges of the plume ranged from 31.9 to 38.5 over a span of approximately 10 km.

3.4. In Situ Salinity Versus Synthetic Salinity Validation

[23] Both the simple and multiple synthetic salinity estimates that used the GSM01 a_{dg} 412 nm data layer predicted

salinity in the region of the CRP with a significant fit of in situ salinity to synthetic salinity measurements and the slopes only moderately deviated from the 1:1 relationship (Table 5 and Figures 9a and 9b). The mean square prediction errors (MSPE) were less than the mean square error (MSE) and therefore the models were effective predictors of salinity. The model estimates using the GSM01 a_{dg} 350 nm data layers produced spurious salinity values for both the 2004 and 2005 data sets (Table 5 and Figures 9c and 9d). Salinity estimates ranged from negative to unrealistically high values; the slopes and intercepts for the validation reveal these extremes (Table 5). Synthetic salinity computed using the GSM01 a_{dg} 412 nm data layer closely approximated in situ salinity, even though the in situ models were
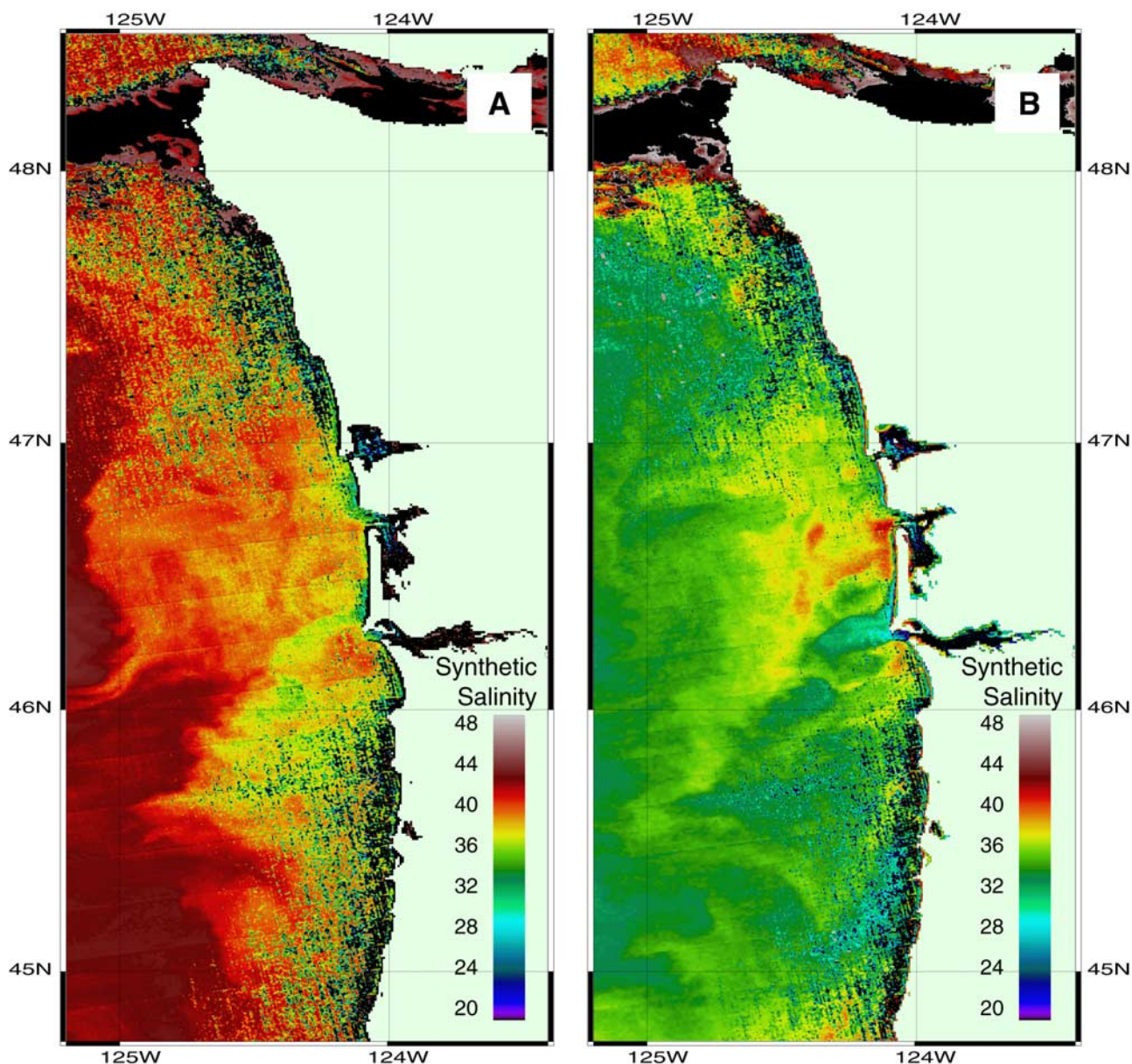
Figure 7. Synthetic salinity. Estimates of sea surface salinity for 25 August 2005, a period of upwelling conditions. (a) Simple algorithm showing salinity versus a_{CDOM} at 350 nm and (b) multiple algorithm showing salinity and temperature versus a_{CDOM} at 350 nm. Satellite products used in analysis included the 250 m MODIS data layers for sea surface temperature and GSM01 a_{dg} 350 nm.

developed using light absorption at 350 nm. This suggests that the GSM01 a_{dg} retrievals are offset (correct spatial pattern, wrong magnitude), reflecting some bias in the GSM01 algorithm. This offset, in addition to limitations in the range of magnitude of underlying data used to develop the synthetic salinity model may explain negative salinity values found in this study. This discrepancy was somewhat present in the model estimates using a_{dg} 412 nm, and extreme for estimates using a_{dg} 350 nm. Therefore, applying the synthetic salinity models to the GSM01 a_{dg} 412 nm data layer instead of a_{dg} 350 nm was the preferred method, and only the validations using the a_{dg} 412 nm method are described.

[24] On 21 July 2004, the simple and multiple models underestimated salinity by approximately 5% and 8%,

respectively (Table 5). The effect of temperature on the multiple algorithm estimate from 2004 was limited because the regression coefficient for temperature was very small ($\beta_2 = 0.01$); for the same reason, estimates from both models are similar. The 25 August 2005 results show wider variability between the two models with the multiple algorithm more closely approximating the in situ salinity measurements (Table 5). The simple algorithm overestimated salinity by 26%. The multiple model overestimated salinity by 10%. The effect of temperature on the multiple algorithm improved the accuracy of the salinity estimates, because the regression coefficient for temperature ($\beta_2 = -0.12$) in the 2005 multiple algorithm was relatively large compared to the 2004 model. Thus, temperature had a larger impact on the fit of modeled to measured salinity in 2005,

Figure 8. Synthetic salinity. Estimates of sea surface salinity for 25 August 2005, a period of upwelling conditions. (a) Simple algorithm showing salinity versus a_{CDOM} at 412 nm and (b) multiple algorithm showing salinity and temperature versus a_{CDOM} at 412 nm. Satellite products used in analysis included the 250 m MODIS data layers for sea surface temperature and GSM01 a_{dg} 412 nm.

an upwelling period. For both the downwelling and upwelling conditions, and despite the uncertainties inherent in this sort of analysis, both algorithms were robust predictors of salinity (MSPE < MSE in all instances).

4. Discussion

[25] The synthetic salinity algorithms developed in this study will permit quantitative observations of the CRP at a higher spatial and temporal resolution than what is currently available by shipboard and mooring observations alone. No previous study has validated satellite imagery of the CRP with in situ, biogeochemically relevant optical properties. These validated algorithms will enable the objective detec-

tion of the plume so that future analyses can describe the geophysical parameters of the plume and not just the location of the putative plume [*Thomas and Weatherbee*, 2006].

[26] The CRP is a dynamic mesoscale feature of the Oregon and Washington shelf. Applying the algorithms of this study to the relatively new 250 m resolution data products from MODIS (B. A. Franz et al., MODIS land bands for ocean remote sensing applications, paper presented at 18th Ocean Optics Meeting, NASA, Montreal, Canada, 2006) was a deliberate choice to spatially resolve fine structure within and near the plume. The gradient in salinity along fronts and the filament extending southwestward from the plume bolus in 2004 (Figure 6) would have

Table 5. Validation of MODIS-Derived Synthetic Salinity Estimates With in Situ Measurements of Salinity for 21 July 2004 and 25 August 2005[a]

| | | | | Results of Regression Analysis | | | Mean Square | |
	Model	r^2	n	β_1	β_0	Mean Square Error	Prediction Errors	p
				21 July 2004				
GSM01 a_{dg} 412 nm	simple	0.89	7	0.95	−0.77	33.28	23.77	<0.05
	multiple	0.89	7	0.92	−0.07	32.37	23.12	<0.05
GSM01 a_{dg} 350 nm	simple	0.89	7	3.42	−100.60	428.10	305.80	<0.05
	multiple	0.89	7	3.39	−99.90	424.80	303.40	<0.05
				25 August 2005				
GSM01 a_{dg} 412 nm	simple	0.85	5	1.26	−0.71	75.86	45.52	<0.05
	multiple	0.87	5	1.10	−1.40	49.10	29.45	<0.05
GSM01 a_{dg} 350 nm	simple	0.85	5	4.50	−117.00	975.60	585.30	<0.05
	multiple	0.86	5	2.95	−67.84	386.80	232.10	<0.05

[a]Synthetic salinity estimates derived from MODIS data layers GSM01 a_{dg} 412 nm and GSM01 a_{dg} 350 nm (β_1 = regression coefficient, β_0 = intercept, and $p \leq 0.05$ is significant).

been poorly resolved in traditional 1 km resolution MODIS data. Data richness increases 16-fold with the new 250 m resolution data products. Although the native resolution is still 1 km for the SST and CDM products, future detailed studies of the fine structure of the plume may be possible; keeping in mind that these products are interpolations of lower-resolution data.

[27] Both empirical algorithms developed in this study generally underestimated salinity during downwelling and overestimated salinity during upwelling, with the multiple algorithm having a closer fit during upwelling. Including temperature in the multiple algorithm conferred an advan-

tage to predicting salinity with more accuracy in 2005 and reduced the detection of false plumes. Existing mooring arrays in the region could be used for near real-time calibration of synthetic salinity computed using daily collections of MODIS-derived a_{dg} 412 nm and SST data layers.

[28] Potential sources of error to explain why synthetic salinity diverges from in situ salinity may be associated with natural variability of the CRP; the default spectral slope parameter used in the GSM01 algorithm to estimate CDM; the offset between a_{CDOM} and a_{dg} estimates; and the quality of the underlying in situ data used to develop the synthetic
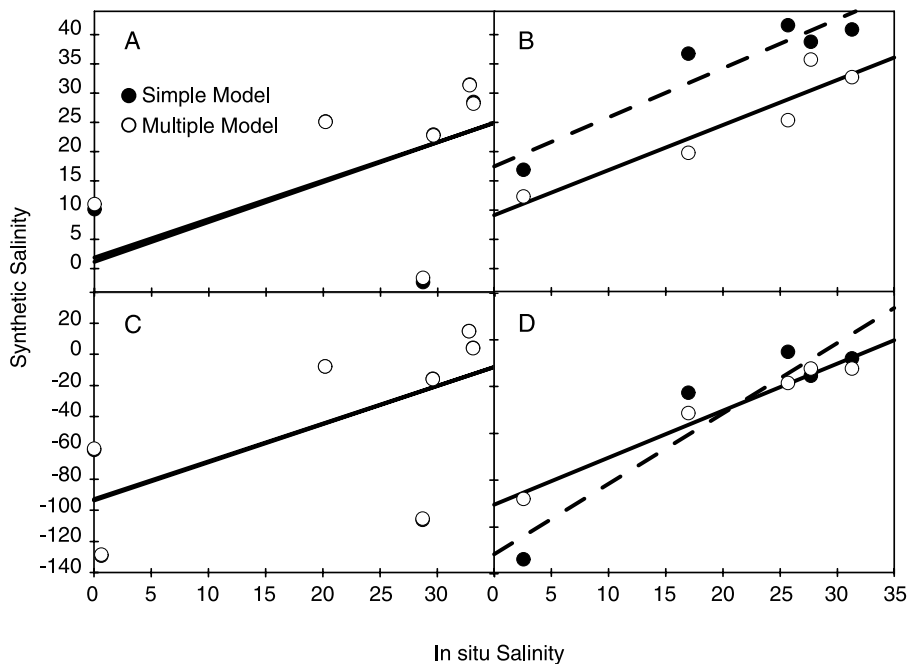
Figure 9. Model validation. Comparison of near-simultaneous (±2 min, 10^6 m^2 grid) MODIS-derived estimates of synthetic salinity and in situ salinity. In situ measurements collected aboard the R/V *Wecoma*, R/V *Point Sur*, and M/V *Forerunner* and via the CoOP-RISE and Columbia River Estuary mooring arrays for (a) 21 July 2004, synthetic salinity from GSM01 a_{dg} 412 nm; (b) 25 August 2005, synthetic salinity from GSM01 a_{dg} 412 nm; (c) 21 July 2004, synthetic salinity from GSM01 a_{dg} 350 nm; and (d) 25 August 2005, synthetic salinity from GSM01 a_{dg} 350 nm. Simple algorithm (solid circles and dashed lines) and multiple algorithm (open circles and dashed lines). See Table 5 for statistics.

salinity models. The CRP is a dynamic feature. In situ measurements used in the salinity validation were limited to a few shipboard and mooring locations. So, all of the variability of the plume may not be captured by these ground truth measurements. Divergence from unity in slopes for both the a_{CDM} versus a_{CDOM} analysis and the salinity comparisons may be partly explained by the decision to use the globally generalized spectral slope parameter, s, employed by GSM01. The global parameter (the default in SeaDAS) overestimates light absorption by CDM in the southern California Current [*Kudela and Chavez*, 2004]. Modifying the algorithm with a spectral slope parameter tuned to the CRP may improve estimates of GSM01 a_{dg} 350 nm, resulting in statistically similar slopes between modeled and measured salinity. However, even regional tuning of s may not substantially improve estimates of CDM [*Kostadinov et al.*, 2007]. Negative synthetic salinity is especially acute in regions where colored detrital material offsets a_{dg} from a_{CDOM} estimates, and is particularly apparent at the mouth of the Columbia River which is a region of sediment resuspension [*Aguilar-Islas and Bruland*, 2006]. CDM includes colloids and detrital material in addition to CDOM. These additional materials could contribute to higher absorption values at 350 nm and 412 nm resulting in specious negative salinity values. Derived satellite estimates for a_{CDOM} relative to total absorption (using the method of *Belanger et al.* [2008]) indicate that detrital material made up to 40% of the a_{dg} 412 nm estimate at the mouth, but only 10% of the estimate in the plume and even less offshore in 2004 (data not shown). Finally, another source of error in the validation may be the quality of data used to develop the synthetic salinity models. A greater number of in situ measurements across the full range of salinity and CDOM concentrations would have improved the models by capturing more of the natural variability of the region. While the relationships deviate from unity both when comparing the simple to multiple models and when validating the model estimates to in situ measurements; all of the salinity comparisons are statistically significant and are useful to describe salinity from ocean color on the Oregon and Washington shelf.

[29] Optical oceanographers have recognized the utility of exploiting the unique optical character of rivers to distinguish them from offshore water [*Binding and Bowers*, 2003; *Callahan et al.*, 2004; *Carder et al.*, 1989; *Hu et al.*, 2004; *Johnson et al.*, 2003; *Conmy et al.*, 2004; *Del Vecchio and Subramaniam*, 2004] and other nearby river plumes [*Chen and Gardner*, 2004]. In the U.S., the Mississippi River plume and the Hudson River plume have been well characterized optically [*Chang et al.*, 2002; *Johnson et al.*, 2003]. Early work in these regions has evolved into more mature studies that integrate physical modeling with optical measurements [*Oliver et al.*, 2004]. Along the New Jersey shore, these models have revealed the varied and sometimes predictable movement of coastal jets [*Chang et al.*, 2002] and upwelling [*Johnson et al.*, 2003]. Predictions of these and other coastal features have improved as a result of the integration of high-resolution physical measurements with in situ and remote optical measurements [*Johnson et al.*, 2003; *Vasilkov et al.*, 1999].

[30] The CRP supplies nitrogen, silica, and trace elements to the coastal margin [*Carpenter and Peterson*, 1989; *Hill and Wheeler*, 2002]. It is an important controller of biomass and primary productivity in the region [*Small and Menzies*, 1981]. Plume-stimulated phytoplankton biomass in this region supports extensive zooplankton populations and juvenile salmon stocks [*De Robertis et al.*, 2005; *Morgan et al.*, 2005]. Phytoplankton productivity is tightly coupled with the physical forcing of upwelling and plume position in this region. Even brief reversals in wind direction can alter the direction of river flow [*Garcia Berdeal et al.*, 2002; *Hickey*, 1998] and this can have an impact on the distribution of standing stocks of biomass. The mechanisms that control the direction of flow and the ultimate fate of the fresh water from the plume continue to be refined [*Garcia Berdeal et al.*, 2002]. The canonical flow hypothesis [*Hickey*, 1979] with northward flow during downwelling-favorable winds, and southwestward flow during upwelling-favorable winds may be an incomplete description of flow. A bifurcated plume or a condition of repeated return into the estuary may be a reality of the CRP that cannot be easily observed and verified from shipboard or drifter measurements alone.

[31] The CRP has historically been described on the basis of salinity [*Hill and Wheeler*, 2002; *Small and Menzies*, 1981]. Previous studies [e.g., *Thomas and Weatherbee*, 2006] have successfully characterized the physical characteristics of the CRP using supervised classification of ocean color data, but were unable to directly link these processes to biogeochemically relevant parameters. Our approach provides a link between the purely statistical methods of *Thomas and Weatherbee* [2006] with the biogeochemically significant parameter: salinity. Increased frequency of observations over larger spatial scales utilizing remote sensing will improve our understanding of CRP flow, delivery of nutrients to the shelf, and residence time of this biological incubator so important to ecosystem health.

References

Aguilar-Islas, A. M., and K. W. Bruland (2006), Dissolved manganese and silicic acid in the Columbia River plume: A major source to the California Current and coastal waters off Washington and Oregon, *Mar. Chem.*, *101*, 233–247, doi:10.1016/j.marchem.2006.03.005.

Babin, M., D. Stramski, G. M. Ferrari, H. Claustre, A. Bricaud, G. Obolensky, and N. Hoepffner (2003), Variations in the light absorption coefficients of phytoplankton, nonalgal particles, and dissolved organic matter in coastal waters around Europe, *J. Geophys. Res.*, *108*(C7), 3211, doi:10.1029/2001JC000882.

Belanger, S., M. Babin, and P. Larouche (2008), An empirical ocean color algorithm for estimating the contribution of chromophoric dissolved organic matter to total light absorption in optically complex waters, *J. Geophys. Res.*, *113*, C04027, doi:10.1029/2007JC004436.

Binding, C. E., and D. G. Bowers (2003), Measuring the salinity of the Clyde Sea from remotely sensed ocean colour, *Estuarine Coastal Shelf Sci.*, *57*, 605–611, doi:10.1016/S0272-7714(02)00399-2.

Blough, N. V., and R. Del Vecchio (2002), Chromophoric DOM in the coastal environment, in *Biogeochemistry of Marine Dissolved Organic Matter*, edited by D. A. Hansell and C. A. Carlson, pp. 509–546, Academic, San Francisco, Calif.

Bricaud, A., A. Morel, and L. Prieur (1981), Absorption by dissolved organic-matter of the sea (yellow substance) in the UV and visible domains, *Limnol. Oceanogr.*, *26*, 43–53.

Callahan, J., M. Dai, R. F. Chen, X. Li, Z. Lu, and W. Huang (2004), Distribution of dissolved organic matter in the Pearl River Estuary, China, *Mar. Chem.*, *89*, 211–224, doi:10.1016/j.marchem.2004.02.013.

Carder, K. L., R. G. Steward, G. R. Harvey, and P. B. Ortner (1989), Marine humic and fulvic acids — Their effects on remote-sensing of ocean chlorophyll, *Limnol. Oceanogr.*, *34*, 68–81.

Carder, K. L., F. R. Chen, Z. P. Lee, S. K. Hawes, and D. Kamykowski (1999), Semianalytic MODIS algorithms for chlorophyll a and absorption with bio-optical domains based on nitrate-depletion temperatures, *J. Geophys. Res.*, *104*, 5403–5421, doi:10.1029/1998JC900082.

Carpenter, R., and M. L. Peterson (1989), Chemical cycling in Washington's coastal zone, in *Coastal Oceanography of Washington and Oregon*, edited by M. R. Landry and B. M. Hickey, pp. 367–485, Elsevier, New York.

Chang, G. C., T. D. Dickey, O. M. Schofield, A. D. Weidemann, E. Boss, W. S. Pegau, M. A. Moline, and S. M. Glenn (2002), Nearshore physical processes and bio-optical properties in the New York Bight, *J. Geophys. Res.*, *107*(C9), 3133, doi:10.1029/2001JC001018.

Chen, R. F., and G. B. Gardner (2004), High-resolution measurements of chromophoric dissolved organic matter in the Mississippi and Atchafalaya river plume regions, *Mar. Chem.*, *89*, 103–125, doi:10.1016/j.marchem.2004.02.026.

Chen, R. F., P. Bissett, P. Coble, R. Conmy, G. B. Gardner, M. A. Moran, X. Wang, M. L. Wells, P. Whelan, and R. G. Zepp (2004), Chromophoric dissolved organic matter (CDOM) source characterization in the Louisiana Bight, *Mar. Chem.*, *89*, 257–272, doi:10.1016/j.marchem.2004.03.017.

Conmy, R. N., P. G. Coble, R. F. Chen, and G. B. Gardner (2004), Optical properties of colored dissolved organic matter in the Northern Gulf of Mexico, *Mar. Chem.*, *89*, 127–144, doi:10.1016/j.marchem.2004.02.010.

Del Vecchio, R., and A. Subramaniam (2004), Influence of the Amazon River on the surface optical properties of the western tropical North Atlantic Ocean, *J. Geophys. Res.*, *109*, C11001, doi:10.1029/2004JC002503.

De Robertis, A., C. A. Morgan, R. A. Schabetsberger, R. W. Zabel, R. D. Brodeur, R. L. Emmett, C. M. Knight, G. K. Krutzikowsky, and E. Casillas (2005), Columbia River plume fronts. II. Distribution, abundance, and feeding ecology of juvenile salmon, *Mar. Ecol. Prog. Ser.*, *299*, 33–44, doi:10.3354/meps299033.

Garcia Berdeal, I., B. M. Hickey, and M. Kawase (2002), Influence of wind stress and ambient flow on a high discharge river plume, *J. Geophys. Res.*, *107*(C9), 3130, doi:10.1029/2001JC000932.

Hernes, P. J., and R. Benner (2003), Photochemical and microbial degradation of dissolved lignin phenols: Implications for the fate of terrigenous dissolved organic matter in marine environments, *J. Geophys. Res.*, *108*(C9), 3291, doi:10.1029/2002JC001421.

Hickey, B. M. (1979), The California Current System — Hypotheses and facts, *Prog. Oceanogr.*, *8*, 191–279, doi:10.1016/0079-6611(79)90002-8.

Hickey, B. M. (1989), Patterns and processes of circulation over the Washington continental shelf and slope, in *Coastal Oceanography of Washington and Oregon*, edited by M. R. Landry and B. M. Hickey, pp. 41–109, Elsevier, New York.

Hickey, B. M., (Ed.) (1998), *Coastal Oceanography of Western North America From the Tip of Baja California to Vancouver Island*, John Wiley, New York.

Hickey, B., A. MacFadyen, W. Cochlan, R. Kudela, K. Bruland, and C. Trick (2006), Evolution of chemical, biological, and physical water properties in the northern California Current in 2005: Remote or local wind forcing?, *Geophys. Res. Lett.*, *33*, L22S02, doi:10.1029/2006GL026782.

Hill, J. K., and P. A. Wheeler (2002), Organic carbon and nitrogen in the northern California Current system: Comparison of offshore, river plume, and coastally upwelled waters, *Prog. Oceanogr.*, *53*, 369–387, doi:10.1016/S0079-6611(02)00037-X.

Hu, C., E. T. Montgomery, R. W. Schmitt, and F. E. Muller-Karger (2004), The dispersal of the Amazon and Orinoco river water in the tropical Atlantic and Caribbean Sea: Observations from space and S-PALACE floats, *Deep Sea Res., Part II*, *51*, 1151–1171.

Johannessen, S. C., W. L. Miller, and J. J. Cullen (2003), Calculation of UV attenuation and colored dissolved organic matter absorption spectra from measurements of ocean color, *J. Geophys. Res.*, *108*(C9), 3301, doi:10.1029/2000JC000514.

Johnson, D. R., J. Miller, and O. Schofield (2003), Dynamics and optics of the Hudson River outflow plume, *J. Geophys. Res.*, *108*(C10), 3323, doi:10.1029/2002JC001485.

Kachel, N. B., and J. D. Smith (1989), Sediment transport and deposition on the Washington continental shelf, in *Coastal Oceanography of Washington and Oregon*, edited by M. R. Landry and B. M. Hickey, pp. 287–365, Elsevier, New York.

Kirk, J. T. O. (1994), *Light and Photosynthesis in Aquatic Ecosystems*, Cambridge Univ. Press, New York.

Klinkhammer, G. P., J. McManus, D. Colbert, and M. D. Rudnicki (2000), Behavior of terrestrial dissolved organic matter at the continent-ocean boundary from high-resolution distributions, *Geochim. Cosmochim. Acta*, *64*, 2765–2774, doi:10.1016/S0016-7037(99)00370-1.

Kostadinov, T. S., D. A. Siegel, S. Maritorena, and N. Guillocheau (2007), Ocean color observations and modeling for an optically complex site: Santa Barbara Channel, California, USA, *J. Geophys. Res.*, *112*, C07011, doi:10.1029/2006JC003526.

Kudela, R. M., and F. P. Chavez (2004), The impact of coastal runoff on ocean color during an El Nino year in Central California, *Deep Sea Res., Part I*, *51*, 1173–1185.

Kudela, R. M., W. P. Cochlan, T. D. Peterson, and C. G. Trick (2006), Impacts on phytoplankton biomass and productivity in the Pacific Northwest during the warm ocean conditions of 2005, *Geophys. Res. Lett.*, *33*, L22S06, doi:10.1029/2006GL026772.

Lagerloef, G., et al. (2008), The Aquarius/SAC-D Mission: Designed to meet the salinity remote-sensing challenge, *Oceanography*, *21*, 68–81.

Landry, M. R., J. R. Postel, W. K. Peterson, and J. Newman (1989), Broad-scale distributional patterns of hydrographic variables on the Washington/Oregon shelf, in *Coastal Oceanography of Washington and Oregon*, edited by M. R. Landry and B. M. Hickey, pp. 1–40, Elsevier, New York.

Lee, Z. P., K. L. Carder, and R. A. Arnone (2002), Deriving inherent optical properties from water color: A multiband quasi-analytical algorithm for optically deep waters, *Appl. Opt.*, *41*, 5755–5772, doi:10.1364/AO.41.005755.

Maritorena, S., D. A. Siegel, and A. R. Peterson (2002), Optimization of a semi-analytical ocean color model for global-scale applications, *Appl. Opt.*, *41*, 2705–2714, doi:10.1364/AO.41.002705.

McCarthy, K. A., and R. W. Gale (1999), Investigation of the distribution of organochlorine and polycyclic aromatic hydrocarbon compounds in the lower Columbia River using semipermeable membrane devices, report, U.S. Geol. Surv., Portland, Oreg.

Mopper, K., and D. J. Kieber (2002), Photochemistry and the cycling of carbon, sulfur, nitrogen and phosphorus, in *Biogeochemistry of Marine Dissolved Organic Matter*, edited by D. A. Hansell and C. A. Carlson, pp. 455–489, Academic, San Francisco, Calif.

Morgan, C. A., A. De Robertis, and R. W. Zabel (2005), Columbia River plume fronts. Hydrography, I., zooplankton distribution, and community composition, *Mar. Ecol. Prog. Ser.*, *299*, 19–31, doi:10.3354/meps299019.

Oliver, M. J., S. Glenn, J. T. Kohut, A. J. Irwin, O. M. Schofield, M. A. Moline, and W. P. Bissett (2004), Bioinformatic approaches for objective detection of water masses on continental shelves, *J. Geophys. Res.*, *109*, C07S04, doi:10.1029/2003JC002072.

Siegel, D. A., S. Maritorena, N. B. Nelson, D. A. Hansell, and M. Lorenzi-Kayser (2002), Global distribution and dynamics of colored dissolved and detrital organic materials, *J. Geophys. Res.*, *107*(C12), 3228, doi:10.1029/2001JC000965.

Small, L. F., and D. W. Menzies (1981), Patterns of primary productivity and biomass in a coastal upwelling region, *Deep Sea Res., Part A*, *28*, 123–149, doi:10.1016/0198-0149(81)90086-8.

Stedmon, C. A., and S. Markager (2003), Behaviour of the optical properties of coloured dissolved organic matter (CDOM) under conservative mixing, *Estuarine Coastal Shelf Sci.*, *57*, 973–979, doi:10.1016/S0272-7714(03)00003-9.

Thomas, A. C., and R. A. Weatherbee (2006), Satellite-measured temporal variability of the Columbia River plume, *Remote Sens. Environ.*, *100*, 167–178, doi:10.1016/j.rse.2005.10.018.

Twardowski, M. S., E. Boss, J. M. Sullivan, and P. L. Donaghay (2004), Modeling the spectral shape of absorption by chromophoric dissolved organic matter, *Mar. Chem.*, *89*, 69–88, doi:10.1016/j.marchem.2004.02.008.

Vasilkov, A. P., V. I. Burenkov, and K. G. Ruddick (1999), The spectral reflectance and transparency of river plume waters, *Int. J. Remote Sens.*, *20*, 2497–2508, doi:10.1080/014311699211895.

R. M. Kudela and S. L. Palacios (corresponding author), Ocean Sciences Department, University of California, Santa Cruz, CA 95064, USA. (spalacio@ucsc.edu)

T. D. Peterson, Division of Environmental and Biomolecular Systems, Department of Science and Engineering, Oregon Health and Science University, 20,000 NW Walker Rd., Beaverton, OR 97006, USA.